

Pressure Influence on the Thermophysical Properties of 316L Austenitic Stainless Steels Manufactured By Powder Metallurgy Method

Ayşe Nur ACAR¹, Abdul Kadir EKŞİ^{*2}, Ahmet EKİCİBİL³

¹Çukurova University, Ceyhan Engineering Faculty, Mechanical Engineering Department Ceyhan Adana

²Çukurova University, Engineering Faculty, Mechanical Engineering Department Sarıçam, Adana

³Çukurova University, Arts and Sciences Faculty, Physical Department Sarıçam, Adana

Geliş tarihi: 08.04.2020

Kabul tarihi: 15.05.2020

Abstract

Austenitic stainless steel that is used in the industrial areas such as automotive has high physical and mechanical properties. In this study; thermophysical properties of 316L austenitic stainless steel prepared by powder metallurgy method that is attracted for researchers due to obtain net or near shaped product and complex shaped materials, have been investigated. Austenitic stainless steels pressed on the 400 and 600MPa pressures and pressed austenitic stainless steel samples sintered at 1200 °C temperature for an hour under inert gas atmosphere. The thermophysical features of these sintered austenitic stainless steel were performed at temperature ranging from RT to 600 °C via heat flux type Differential Scanning Calorimeter (DSC). These properties supported by SEM images, EDS spectrums and OM (Optic microscope) images.

Key Words: Specific heat capacity, Enthalpy, Austenitic stainless steel, Powder metallurgy

Toz Metalurjisi ile Üretilen 316L Östenitik Paslanmaz Çeliklerin Termofiziksel Özelliklerin Üzerindeki Basıncın Etkisi

Öz

Otomotiv gibi endüstriyel alanlarda kullanılan östenitik paslanmaz çelik yüksek fiziksel ve mekaniksel özelliklere sahiptir. Bu çalışmada benzer ya da benzere yakın şekilli ürün ve karmaşık şekilli malzeme üretilmesine olanak sağlanmasından dolayı araştırmacılar tarafından cazip görülen toz metalurjisi yöntemiyle hazırlanan 316L östenitik paslanmaz çeliğin termofiziksel özellikleri araştırılmıştır. Östenitik paslanmaz çelikler 400 ve 600 MPa basınçlarında preslenmiş ve preslenen östenitik paslanmaz çelik numuneler 1200 °C sıcaklığında 1 sa boyunca inert gaz atmosferinde sinterlenmiştir. Bu sinterlenmiş östenitik paslanmaz çeliklerin termofiziksel özellikleri oda sıcaklığından 600 °C'ye kadar olan sıcaklık aralığında ısı akışı tipli Diferansiyel Taramalı Kalorimetreye (DSC) ile ölçülmüştür. Bu özellikler SEM görüntüleri, EDS spektrumları ve OM (optik mikroskop) görüntüleri ile desteklenmiştir.

Anahtar Kelimeler: Özgül ısı kapasitesi, Entalpi, Östenitik paslanmaz çelik, Toz metalurjisi

*Sorumlu yazar (Corresponding author): Abdul Kadir EKŞİ, akeksi@cu.edu.tr

1. INTRODUCTION

Thermophysical properties of materials are varied with temperature but not cause to changes on the chemical properties of materials. Specific heat capacity and enthalpy features are thermophysical properties of materials. Specific heat capacity is needed heat amount to increase temperature of 1 g of materials by 1 °C and enthalpy is internal energy of materials [1,2,3]. Specific heat capacity and enthalpy of materials features are calculated following formulas [2,4] (Equations 1 and 2);

$$C_p = c_0 + c_1 T + c_2 T^2 + c_3 T^3 \quad (1)$$

$$\Delta H = \int c_p dT \quad (2)$$

Equation (1) formularizes specific heat capacity of materials and Equation (2) is obtained by integrated of specific heat capacity of materials and formularizes enthalpy behaviours of materials. On the Equations (1) and (2); c_0 , c_1 , c_2 , c_3 are coefficients of specific heat capacity of elements and T is temperature. c_p and ΔH are referred as specific heat capacity and enthalpy symbols [2,4].

Powder metallurgy used in widely applied in the industrial areas provides to obtain similar or near to similar shaped products and high physical properties owing to closing porosity and grain bonding by method's very nature. On the method; powder /powder preparation, compaction of powder /powder mixture and sintering of compacted green bulk products are stages of this method. Sintered bulk products have more strengthening structure according to green bulk products [5-9].

In this study; specific and heat capacity and enthalpy behaviours of 316L austenitic stainless steel samples that is widely used in industrial areas and has low amounts of carbon, charomium, nickel and molybdenum, have been examined.

2. MATERIAL AND METHOD

In this study; 316L austenitic powder that obtained from North American Höganäs, Co. utilized the

chemical composition (wt%) of this powder consists of 16.41 of Cr, 13.18 of Ni, 2.17 of Mo, 0.98 of Si, 0.23 of Mn, 0.02 of C, 0.018 of P, balance of Fe and 1.0 of acrawax as binder; and mean particle size distribution of this powder is 14.04 μm . This austenitic stainless steel powder pressed on the 400 and 600 MPa pressures using traditional pressing technique. Pressed stainless steel compacts sintered according to heat treatment cycle specified in Figure 1. Sintering process happened under Ar atmosphere. Firstly samples annealed at 600 and 900 °C temperatures for 30 min in order to provide debind of grains in the green bulk product and unifom temperature distribution in the furnace according to literature [10-12]. After then, samples sintered at 1200 °C temperature for an hour. Heating and cooling rate were selected as 5 °C/min. The thermophysical features o these sintered austenitic stainless steels were performed at temperature ranging from RT to 600 °C via heat flux type Differential Scanning Calorimeter (DSC) using N_2 of gas, 20 mL/min of gas flow and 20°C/min of gas rate.

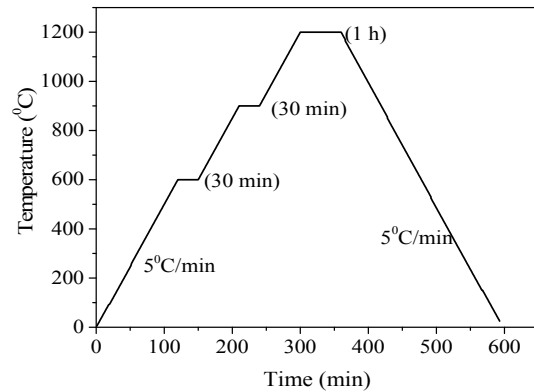


Figure 1. The heat treatment cycle

3. RESULTS AND DISCUSSION

The SEM image and particle size distribution of 316L austenitic stainless steel powder were showed in Figure 2. According to SEM image of this powder; particle size of powder has irregular shape that type of water atomized particle and particle size distribution of this powder showed the positively skewed particle size distribution due to mostly fine particles into the alloy [13-15].

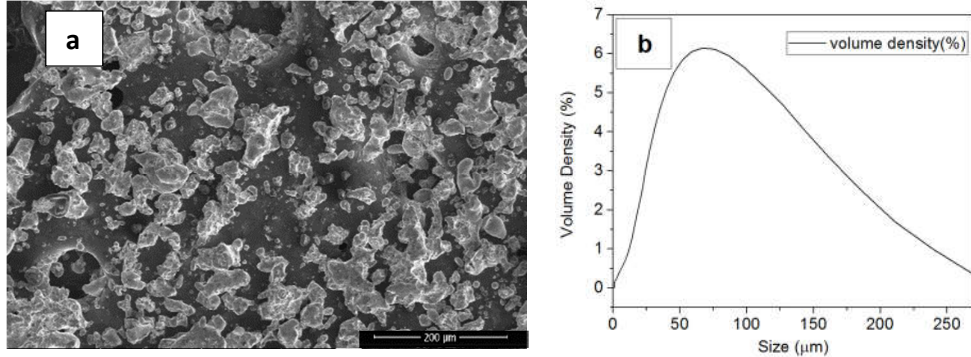


Figure 2. The SEM Image and particle size distribution of 316L austenitic stainless steel powder

Figure 3 and Figure 4 shows the specific heat capacity ($J/g^{\circ}C$) –temperature ($^{\circ}C$) and enthalpy (J/g) –temperature ($^{\circ}C$) curves of sintered 316L austenitic stainless steel samples. As seen in Figure 3; when temperature increased; specific heat capacity and enthalpy values increased but not perfect linearly increase due to rising of amplitude of atomic vibration of the stainless steels’s composition with rising temperature [16]. On the austenitic stainless steel prepared on the 600 MPa pressure; when increasing temperature from 300 $^{\circ}C$ temperature; specific heat capacity values of this material decreased. As pressure increased; specific heat capacity and enthalpy of these austenitic stainless steel samples decreased. This situation can be recommended that occurring of reaction between alloying elements and carbon happens a liquid phase. This phase leads to densification [17]. Much carbon existence on the stainless steel prepared on the 400 MPa pressure play a role on the occurring of transformation of martensitic structure [18]. Porosity existence were appeared on both of austenitic stainless steel. Austenitic stainless steel prepared on the 400 MPa pressure has more porosity than that of other stainless steel. This situation can be considered that porosity existence and martensitic structure have decreasing effect on the both of specific heat capacity and enthalpy values of 316L austenitic stainless steels with increasing of pressure. As carefully examining of specific heat capacity values of both of austenitic stainless steel prepared on the 400 and 600 MPa pressures; frustrating was observed at temperature ranges from ≈ 100 to ≈ 200 $^{\circ}C$, it can be considered that this situation is

exothermic peak and it can be commented that this peak is resulted increasing from minor precipitation during heat treatment cycle on the manufacturing process [19].

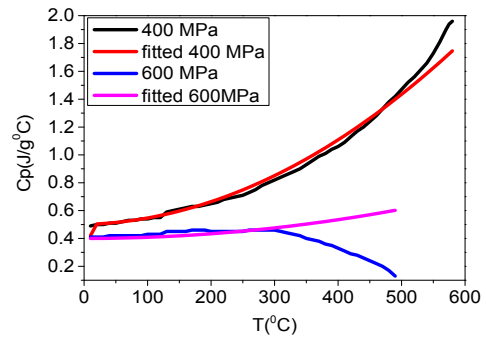


Figure 3. The specific heat capacity ($J/g^{\circ}C$)–temperature ($^{\circ}C$) curves of sintered 316L austenitic stainless steel samples

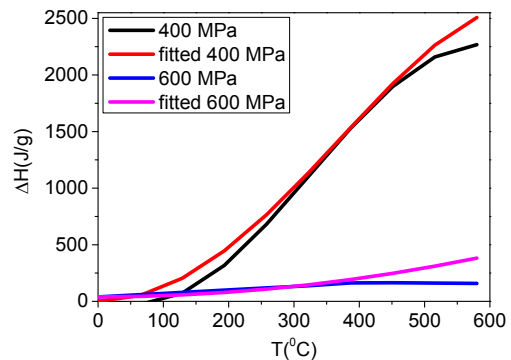


Figure 4. The enthalpy (J/g) –temperature ($^{\circ}C$) curves of sintered 316L austenitic stainless steel samples

Maximum specific heat capacity and enthalpy obtained on the austenitic stainless steel prepared on the 400 MPa pressure (013 J/ g°C at 490°C and 2268.2 J/g at 580 °C, respectively). On the Tables 1 and 2; specific heat capacity and enthalpy values of these austenitic stainless steel samples are given with fitted values and errors (%) and on the Tables 3 and 4; the fit coefficients and

nonlinear square regression values of austenitic stainless steel samples are given by helping of Microsoft Excel Office program. According to these square regression values; the best fit obtained on the austenitic stainless steel prepared on the 400 MPa pressure for specific heat capacity and enthalpy behaviours ($R^2= 0.9494$ and 1.00 for specific heat capacity and enthalpy, respectively).

Table 1. The specific heat capacity v.s. Temperature values of 316L austenitic stainless steels

T(°C)	c_p (J/g°C) (400 MPa)	Fitted c_p (J/g°C) (400MPa)	Error(%)	c_p (J/g°C) (600 MPa)	Fitted c_p (J/g°C) (600MPa)	Error(%)
10	0.49	0.42	-14.2857	0.41	0.400092	-2.41659
20	0.5	0.50380	0.760225	0.41	0.400352	-2.35317
30	0.5	0.506750	1.350067	0.41	0.40078	-2.24878
40	0.51	0.51040	0.078459	0.42	0.401376	-4.43429
50	0.51	0.514750	0.931387	0.42	0.40214	-4.25238
60	0.52	0.519800	-0.03845	0.42	0.403072	-4.03048
70	0.53	0.525550	-0.83962	0.42	0.404172	-3.76857
80	0.53	0.532000	0.377362	0.42	0.40544	-3.46667
90	0.54	0.539150	-0.15741	0.42	0.406876	-3.12476
100	0.54	0.54700	1.296298	0.43	0.40848	-5.00465
110	0.55	0.555550	1.009092	0.43	0.410252	-4.59256
120	0.55	0.564800	2.69091	0.43	0.412192	-4.1414
130	0.59	0.574750	-2.158475	0.45	0.4143	-7.93333
140	0.6	0.585400	-2.43333	0.45	0.416576	-7.42756
150	0.61	0.596750	-2.17213	0.45	0.41902	-6.88444
160	0.62	0.608800	-1.80645	0.45	0.421632	-6.304
170	0.63	0.621550	-1.34127	0.46	0.424412	-7.73652
180	0.63	0.63500	0.793651	0.46	0.42736	-7.09565
190	0.64	0.64915	1.429688	0.46	0.430476	-6.41826
200	0.65	0.66400	2.153846	0.45	0.43376	-3.60889
210	0.66	0.679550	2.962121	0.45	0.437212	-2.84178
220	0.68	0.695800	2.32353	0.45	0.440832	-2.03733
230	0.69	0.712750	3.297102	0.45	0.44462	-1.19556
240	0.7	0.73040	4.342857	0.45	0.448576	-0.31644
250	0.71	0.74875	5.457747	0.45	0.4527	0.6
260	0.73	0.7678	5.178082	0.46	0.456992	-0.65391
270	0.75	0.78755	5.006667	0.46	0.461452	0.315652
280	0.78	0.808	3.589744	0.46	0.46608	1.321739
290	0.8	0.82915	3.64375	0.46	0.470876	2.364348
300	0.82	0.851	3.780488	0.46	0.47584	3.443478
310	0.84	0.87355	3.994048	0.45	0.480972	6.882667
320	0.86	0.8968	4.27907	0.44	0.486272	10.51636
330	0.88	0.92075	4.630682	0.43	0.49174	14.35814
340	0.9	0.9454	5.044444	0.42	0.497376	18.42286
350	0.93	0.97075	4.38172	0.4	0.50318	25.795
360	0.96	0.9968	3.833333	0.39	0.509152	30.55179
370	0.99	1.02355	3.388889	0.38	0.515292	35.60316
380	1.01	1.051	4.059406	0.36	0.5216	44.88889
390	1.04	1.07915	3.764423	0.35	0.528076	50.87886
400	1.06	1.108	4.528302	0.33	0.53472	62.03636
410	1.09	1.13755	4.362385	0.31	0.541532	74.68774

420	1.13	1.1678	3.345133	0.29	0.548512	89.14207
430	1.17	1.19875	2.457265	0.28	0.55566	98.45
440	1.2	1.2304	2.533333	0.26	0.562976	116.5292
450	1.24	1.26275	1.834677	0.24	0.57046	137.6917
460	1.28	1.2958	1.234375	0.22	0.578112	162.7782
470	1.33	1.32955	-0.03383	0.2	0.585932	192.966
480	1.38	1.364	-1.15942	0.17	0.59392	249.3647
490	1.42	1.39915	-1.46831	0.13	0.602076	363.1354
500	1.47	1.435	-2.38095			
510	1.52	1.47155	-3.1875			
520	1.56	1.5088	-3.28205			
530	1.61	1.54675	-3.92857			
540	1.66	1.5854	-4.49398			
550	1.73	1.62475	-6.08382			
560	1.81	1.6648	-8.0221			
570	1.9	1.70555	-10.2342			
575	1.94	1.7261875	-11.0213			

Table 2. The Enthalpy v.s. temperature values of 316L austenitic stainless steels

T (°C)	ΔH (J/g) (400 MPa)	Fitted ΔH (J/g) (400MPa)	Error (%)	ΔH (J/g) (600 MPa)	Fitted ΔH (J/g) (600MPa)	Error (%)
0	-0.83	0.0001	-100.012	39.17	39	-0.43401
64.45	29.14	51.66382	-277.295	59.24	43.79919	-26.0648
128.9	72.24	203.5493	181.7681	79.26	56.91135	-28.1966
193.35	317.86	446.3392	40.42006	99.16	78.34182	-20.9945
257.8	681.18	764.505	12.23245	118.88	108.096	-9.07137
322.25	1105.17	1136.307	2.817357	137.83	146.1791	6.057541
386.7	1529.15	1533.792	0.303585	162.78	192.5966	18.31714
451.15	1897.55	1922.799	1.330613	164.48	247.3539	50.3854
515.69	2159.43	2263.372	4.813409	161.31	310.5502	92.51764
580.05	2268.2	2507.666	10.55754	158.15	381.909	141.4853

Table 3. The fit coefficients and nonlinear-squares regression values of specific heat capacity behaviour of 316L austenitic stainless steel samples

	316L/400 MPa	316L/600 MPa
c_0	0.5	0.4
c_1	0.00012	0.0000008
c_2	0.0000035	0.00000084
c_3	0.009	0.0000003
R^2	0.9494	0.9401

Table 4. The fit coefficients and nonlinear-squares regression values of enthalpy behaviour of 316L austenitic stainless steel samples

	316L/400 MPa	316L/600 MPa
c_0	4.00E-01	0.5
c_1	0.00000012	0.0011
c_2	9.00E-12	9E-12
c_3	0	0
c_4	3.90E+01	70
R^2	1.00	0.9882

In Figure 5; the enthalpy ($\Delta H_T - \Delta H_{298}^{\circ}$)-temperature curves of 316L austenitic stainless steel samples were shown with experimental and fitted enthalpy values. The enthalpy ($\Delta H_T - \Delta H_{298}^{\circ}$) v.s. temperature values of 316L austenitic stainless steels were given in Table 5.

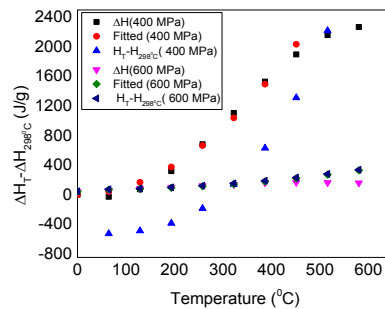


Figure 5. The Enthalpy enthalpy ($\Delta H_T - \Delta H_{298}^{\circ}$) (J/g)-temperature (°C) curves of sintered 316L austenitic stainless steel samples

In Figure 6; the SEM images of 316L austenitic stainless steels prepared on 400 and 600 MPa pressures observed. From Figure 6, it was observed that when pressure increased, closing porosity and grain bonding observed. On the austenitic stainless steel prepared on the low pressure; liquid phase formation among grains was clearly seen. It can be commented that higher specific heat capacity and enthalpy values of this austenitic stainless steel sample values than that of other austenitic stainless steel resulted from this situation. It was also seen and considered that ferrite grains and austenite matrix are also

observed. On the Table 6, the EDS spectrums of both of austenitic stainless steels samples are given. From EDS spectrums; it was appeared that all alloying elements homogeneously dispersed on the surface of both of stainless steel samples and carefully examined that Si alloying element on the austenitic stainless steel samples prepared on the low pressure has higher than that of other austenitic stainless steel sample. Si has a significant role on the stabilizing ferritic structure and enhances the thermophysical properties of austenitic stainless steel samples [20].

Table 5. The Entalpy ($\Delta H_T - \Delta H_{298}^0$) v.s. temperature values of 316L austenitic stainless steels

T (°C)	ΔH (J/g) (400 MPa)	Fitted ΔH (J/g) (400MPa)	$\frac{\Delta H_T - \Delta H_{298}^0}{\Delta H_{298}^0}$ (J/g) (400 MPa)	ΔH (J/g) (600 MPa)	Fitted ΔH (J/g) (600MPa)	$\Delta H_T - \Delta H_{298}^0$ (J/g) (600 MPa)
0.01	-0.83	-1.8785	-802.079	39.17	42.50002695	45.03376
64.45	-29.14	41.53453	-762.137	59.24	67.940832	71.61114
128.9	72.24	166.1486	-649.927	79.26	76.90174504	81.54315
193.35	317.86	373.8388	-462.949	99.16	92.12903468	98.07982
257.8	681.18	664.605	-201.205	118.88	113.8689965	121.2212
322.25	1105.17	1038.447	135.3063	137.83	142.3679261	150.9673
386.7	1529.15	1495.366	546.5834	162.78	177.8721189	187.3183
451.15	1897.55	2035.36	1032.626	164.48	220.6278706	230.2741
515.69	2159.43	2659.359	1594.269	161.31	270.9570098	279.9087
580.05	2268.2	3364.577	2229.006	158.15	328.8792329	336.0006

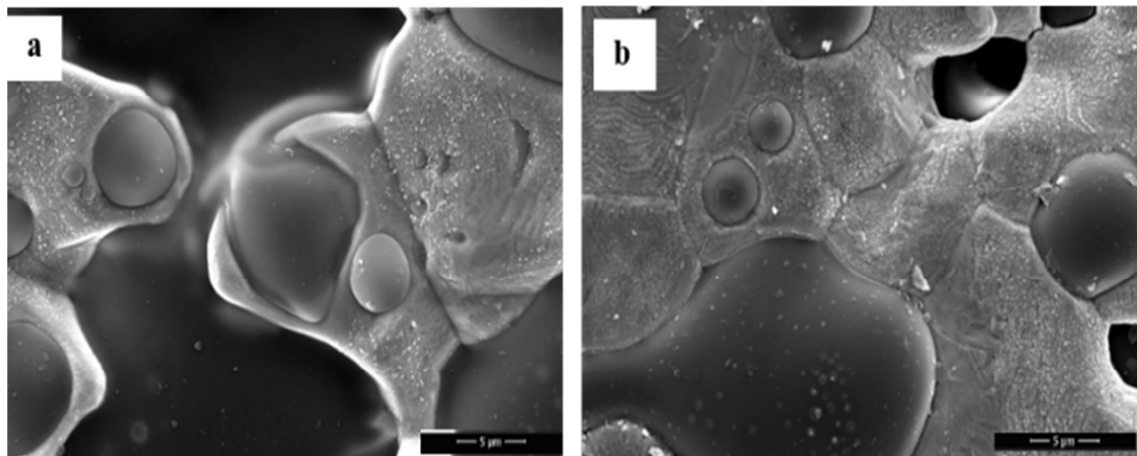


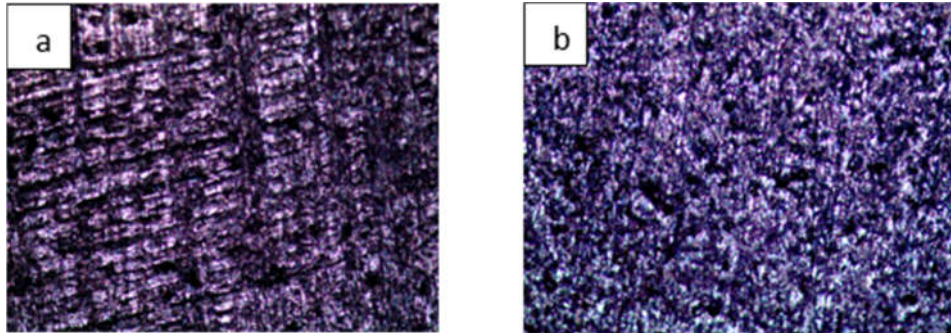
Figure 6. The SEM Images of 316L austenitic stainless steel prepared on 400 (a) and 600 (b) pressures

Table 6. The EDS spectrums of 316L austenitic stainless steels

		316L /400 MPa		316L/ 600 MPa	
	Element	Weight %	Atomic%	Weight %	Atomic%
Spectrum 1	Cr	16.89	17.97	16.53	15.25
	Fe	67.44	66.82	68.87	59.14
	Ni	12.01	11.32	12.24	10.00
	Mo	2.40	1.38	1.67	0.83
	Si	1.26	2.50	0.68	1.17
Spectrum 2	Cr	16.01	15.46	15.52	14.19
	Fe	64.02	57.52	69.85	58.97
	Ni	11.04	9.43	12.20	9.87
	Mo	2.18	1.14	1.66	0.82

Figure 7 shows OM (optic microscope) images of both of austenitic stainless steel samples; OM images showed that both of 316L austenitic stainless steels have uniform surfaces. Pressure effect observed on the decreasing porosity and occurring of grain bonding with grain binding. [21]. According to literature; microstructures of

both austenitic stainless steels having uniform surfaces involves of austenitic matrix and indiscriminately disrupted ferritic grains throughout grains [22-24]. This case also observed on the SEM images of these stainless steel samples.

**Figure 7.** The OM Images of 316 austenitic stainless steel prepared on 400 (a) and 600 (b) pressures

4. CONCLUSION

In this study; the thermophysical properties of PM-316L austenitic stainless steel compacts were investigated. Following experimental results are given.

1. As temperature increased, specific heat capacity and enthalpy properties of stainless steels increased.
2. As pressures increased, these properties of stainless steels are decreased.

3. On the SEM images and OM images; ferritic grains and austenitic matrix observed.

5. ACKNOWLEDGEMENT

This study is financially supported by Çukurova University Research Funding (FBA-2018-11074).

6. REFERENCES

1. Morintale, E., Harabor, A., Constantinescu, C., Rotaru, P., 2015. Use of Heat Flows from DSC

- Curve for Calculation of Specific Heat of the Solid Materials, Physics AUC. 23, 89-94.
2. Wielgosz, E., Kargul, T., Falkus, J., 2014. Comparison of Experimental and Numerically Calculated Thermal Properties of Steels, International Conference on Metallurgy and Materials, Metal 2014, May 21st-23rd 2014, Brno, Czech Republic.
 3. Fang, H., Wong, M.B., Bai, Y., 2015. Use of Kinetic Model for Thermal Properties of Steel at High Temperatures, Australian Journal of Civil Engineering, 13(1), 40-47.
 4. Kelley, K.K., 1949. X. High-Temperature Heat-Content, Heat-Capacity, and Entropy Data for Inorganic Compounds, Bureau of Mines Bull. 476, 192.
 5. Acar, A.N., Ekşi, A.K., Ekicibil, A., 2019. Effect of Pressure on the Magnetic and Structural Properties of X2CrNiMo17-12-2 Austenitic Stainless Steel Prepared by Powder Metallurgy Method Journal of Molecular Structure, 1198, 126876.
 6. Acar, A.N., Mutlu, R.N., Ekşi, A.K., Ekicibil, A., Yazıcı, B., 2018. Effect of Temperature and Pressure on Mechanical, Surface and Electrochemical Properties of Al-1.5Cu-5.5Zn-2.5Mg (Alumix-431), Anti-Corrosion Methods and Materials 65/6, 558–571.
 7. Akhavan Tabatabae, B., Ashrafizadeh, F., Hassanlı, A.M., 2011. Influence of Retained Austenite on the Mechanical Properties of Low Carbon Martensitic Stainless Steel Castings, ISIJ International, 51(3), 471–475.
 8. Azevedo, J.M.C., Serrenho, A.C., Allwood, J.M., 2018. Energy and Material Efficiency of Steel Powder Metallurgy, Powder Technology 328, 329–336.
 9. Kulkarni, H., Dabhade, V.V., 2019. Green Machining of Powder-Metallurgy-Steels (PMS): An Overview, Journal of Manufacturing Processes 44, 1–18.
 10. Butković, S., Oruč, M., Šarić, E., Mehmedović, M., 2012. Effect of Sintering Parameters on the Density, Microstructure and Mechanical Properties of the Niobium-Modified Heat-Resistant Stainless Steel GX40CrNiSi25-20 Produced by MIM Technology, Materiali in tehnologije/Materials and technology 46(2), 185-190.
 11. Butković, S., 2013. Sinterability and Tensile Properties of Nickel Free Austenitic Stainless Steel X15CrMnMoN 17 11 3, Tehnički vjesnik (Technical Gazette) 20(2), 269-274.
 12. Pandya, S., Ramakrishna, K.S., Annamalai, A.R., Upadhyaya, A., 2012. Effect of Sintering Temperature on the Mechanical and Electrochemical Properties of Austenitic Stainless Steel, Materials Science and Engineering A 556, 271–277.
 13. Rudianto, H., Jang, G., Yang, S., Kim, Y., Dlouhy, I., 2015. Effect of SiC Particles on Sinterability of Al-Zn- Mg-Cu P/M Alloy”, Archives of Metallurgy and Materials, 60(2), 1383-1385.
 14. Rudianto, H., Jang, G.J., Yang, S.S., Kim, Y.J. Dlouhy, I. (2015b). Evaluation of Sintering Behavior Of Premix Al-Zn- Mg-Cu Alloy Powder”, Advances in Materials Science and Engineering, Article ID 987687, 8.
 15. Dyankova, S., Doneva, M., Todorov, Y., Terziyska, M., 2016. Determination of Particle Size Distribution and Analysis of a Natural Food Supplement on Pectin Base, IOSR Journal of Pharmacy, 6(5), 01-08.
 16. Karthikeyan, B., Ramanathan, S., Ramakrishnan, V., 2010. A Calorimetric Study of 7075 Al/SiCp Composites, Materials and Design, 31, 92–95.
 17. Karwan-Baczewska, J., 2015. Processing and Properties of Distaloy SA Sintered Alloys with Boron and Carbon, Archives of Metallurgy and Materials, 60(1), 41-45.
 18. Abdoos, H., Khorsand, H., Shahani, A.R., Fatigue Behavior of Diffusion Bonded Powder Metallurgy Steel with Heterogeneous Microstructure, Materials and Design 30, 1026-1031.
 19. Wilthan, B., Reschab, H., Tanzer, R., Schützenhöfer, W., Pottlacher, G., 2008. Thermophysical Properties of Chromium-Nickel-Molybdenum Steel in the Solid and Liquid Phases, Int. J. Thermophys., 29, 434-444.
 20. Isfahany, A.N., Saghafian, H., Borhani, G., 2011. The Effect of Heat Treatment on Mechanical Properties and Corrosion Behaviour of AISI420 Martensitic Stainless

- Steel, Journal of Alloys and Compounds 509, 3931–3936
21. Acar, A.N., 2019. Investigation of Physical and Mechanical Properties of 316L and 410 Stainless Steels Manufactured by Powder Metallurgy Method Doctoral Thesis, Çukurova University, Institute of Natural and Applied Sciences, 139.
 22. Moteshakker, A., Danaee I., 2016. Microstructure and Corrosion Resistance of Dissimilar Weld-Joints between Duplex Stainless Steel 2205 and Austenitic Stainless Steel 316L Moteshakker, A., Danaee I., Journal of Materials Science and Technology, 32, 282-290.
 23. Mamat, M.F., Hamzah E., Ibrahim, Z., Rohah, A.M., Bahador, A., 2015. Effect of Filler Metals on the Microstructures and Mechanical Properties of Dissimilar Low Carbon Steel and 316L Stainless Steel Welded Joints, Materials Science Forum, 819, 57-62.
 24. Simionescu, N., Benea, L., Dumitrascu, V.M., 2018. The Synergistic Effect of Proteins and Reactive Oxygen Species on Electrochemical Behaviour of 316L Stainless Steel for Biomedical Applications, IOP Conf. Series: Materials Science and Engineering, 374 Euroinvent ICIR 2018 17–18 May 2018, Iasi, 1-7, Romania.

